Received: 15 December 2020 | Revised: 8 June 2021 | Accepted: 3 July 2021

DOI: 10.1111/apha.13715

SIGNALLING

ACTA PHYSIOLOGICA

Calcineurin (PPP3CB) regulates angiotensin II-dependent vascular remodelling by potentiating EGFR signalling in mice

Alexander Nolze | **Conny Köhler** | **Stefanie Ruhs** | **Katja Quarch** | **Nicole Strätz** | **Michael Gekle** | **Claudia Grossmann**

Julius-Bernstein-Institute of Physiology, Martin Luther University Halle-Wittenberg, Halle, Germany

Correspondence
Claudia Grossmann, Julius-Bernstein-Institute of Physiology, Martin Luther University Halle-Wittenberg, Magdeburger Str. 6, Halle (Saale) 06112, Germany.
Email: claudia.grossmann@medizin.uni-halle.de

Funding information
Wilhelm-Roux-Program, Grant/Award Number: FKZ: 28/30; Deutsche Forschungsgemeinschaft, Grant/Award Number: GE 905/19-1

Abstract

Aim: This study investigates the role of calcineurin for angiotensin II (AngII)-induced vascular remodelling with the help of a mouse model lacking the catalytic beta subunit of calcineurin (PPP3CB KO).

Methods: Wildtype (WT) and PPP3CB KO mice were treated for 4 weeks with AngII followed by assessment of blood pressure, histological evaluation of aortas and mRNA analysis of aortic genes PPP3CB-dependently regulated by AngII. Primary murine vascular smooth muscle cells (VSMCs) were used for qPCR, ELISA and Western Blot experiments as well as wound healing and cell proliferation assays.

Results: Upon AngII treatment, PPP3CB KO mice showed less aortic media thickening, lumen dilation and systolic blood pressure compared to WT mice. Next-generation sequencing data of aortic tissue indicated an increase in extracellular matrix components (EMCs), cell migration and cell proliferation. A PPP3CB-dependent increase in EMC was confirmed by qPCR in aorta and VSMCs. PPP3CB-dependent stimulation of VSMC migration could be verified by wound healing assays but markers of enhanced cell proliferation were only detectable in aortic tissue of WT mice but not in isolated WT or KO VSMCs. We could demonstrate in VSMCs with pharmacological inhibitors that PPP3CB leads to enhanced heparin-binding EGF-like growth factor (HB-EGF) secretion, epidermal growth factor receptor (EGFR) activation and consecutive stimulation of transforming growth factor β(TGFβ) and connective tissue growth factor (CTGF) signalling that enhances collagen expression.

Conclusion: AngII-induced vascular remodelling involves PPP3CB, which leads to enhanced EMC production, VSMC migration and sustained increase in systolic blood pressure via HBEGF/EGFR-TGFβ-CTGF signalling.

KEYWORDS

angiotensin II, calcineurin, EGFR, remodelling, vasculature

1 | INTRODUCTION

Vascular remodelling is a hallmark of cardiovascular diseases and shows a strong correlation with inappropriate activation of the renin-angiotensin system (RAS). Activation of the angiotensin II-type 1 (AT_1) receptor by AngII has been implicated to alter vascular tone and favour tissue remodelling as it promotes vascular smooth muscle cell (VSMC) migration and senescence, vascular hypertrophy, endothelial dysfunction, oxidative stress as well as synthesis and release of extracellular matrix proteins.[1-3] Some reports also suggest that dysregulation of AngII signalling contributes to increased inflammation.[4-6] Besides binding to AT1 receptors, AngII can also bind to AT2 receptors, which mediate opposite effects and cause vasodilation as well as antifibrotic and antiinflammatory effects. Another possibility is that AngII enzymatically gets converted to Ang(1-7) and then binds to the Mas receptor, a G protein-coupled receptor that also exerts inhibitory effects on fibrosis, hypertrophy and inflammation.[7] For the pathological AngII-mediated effects, the detailed pathogenic molecular mechanisms remain elusive. Here, we investigate the role of the phosphatase calcineurin for AngII-dependent vascular changes with the help of a global KO model for the catalytic beta subunit of calcineurin (PPP3CB).

Calcineurin belongs to the family of the Ca^{2+}/calmodulin-dependent serine/threonine protein phosphatases consisting of catalytic (PPP3C) and regulatory (PPP3R) subunits, which are both expressed as multiple isoforms.[8,9] PPP3C is encoded by three distinct genes, PPP3CA, PPP3CB and PPP3CC, of which PPP3CA and PPP3CB are ubiquitously expressed, whereas PPP3CC is restricted to the testis and a limited region of the brain.[10,11] The regulatory subunit PPP3R, which directs the substrate specificity of the catalytic subunit, is encoded by two genes, PPP3R1 and PPP3R2.[12] Calcineurin is known for dephosphorylating different transcription factors with pathophysiological relevance for remodelling-associated processes including inflammation, hypertrophy and autophagy. For example, it can dephosphorylate and thereby inactivate the transcription factor CREB, which leads to shortening of life span and reduced reactive oxygen species (ROS) scavenging capacity.[13,14] On the other hand, NFaT (nuclear factor of activated T cells) signalling is activated by calcineurin and plays a role in immune responses, hypertrophy of skeletal and cardiac muscles and also in the developmental processes of the cardiovascular system.[15-20] Calcineurin is also important for angiogenesis and vascular branching and global inactivation of PPP3, for example by inactivation of the regulatory calcineurin subunit PPP3R1, causes embryonic lethality because of the failure of vascular patterning in the mouse embryo.[17,21] Experiments with the calcineurin inhibitors cyclosporine A and FK506 indicate that calcineurin may also play an important role in the pathogenesis of vascular diseases like hypertension, atherosclerosis and vascular remodelling but the exact nature of these effects, the calcineurin subunit isoforms involved and the underlying mechanisms are still controversial.[22-24]

The influence of AngII on calcineurin activity has been especially well demonstrated in the heart. Mice with reduced PPP3CB activity showed a decreased hypertrophic growth response upon AngII infusion or pressure overload.[25] On the other hand, a loss of PPP3CB increased the sensitivity of the myocardium to ischaemia-reperfusion injury, implying a positive effect of calcineurin signalling in myocyte viability maintenance.[26] Additionally, calcineurin inhibition influences AngII-induced neointima and aneurysm formation in the mouse models of vascular injury or atherosclerosis.[27] These findings indicate a putative interaction between the RAS and calcineurin especially in terms of pathological tissue remodelling.

Another important signalling pathway that can be stimulated by AngII is epidermal growth factor receptor (EGFR) signalling.[28] It is known that canonical EGFR activation or transactivation can activate extracellular signal-regulated kinases 1/2 (ERK1/2) or phosphatidylinositol 3-kinase/protein kinase B (PI3K/Akt) signalling.[29] Transactivation of EGFR can occur via heparin-binding EGF-like growth factor (HBEGF). It was shown that a blockage of HBEGF-mediated EGFR transactivation abolishes AngII-induced cardiac hypertrophy.[30] In another study, inhibition of EGFR signalling in VSMCs led to a reduction of AngII-induced end organ damage.[31] Despite the importance of AngII in cardiovascular dysfunction and remodelling, the signalling pathways regulating these processes have not been completely elucidated.

In this study, we therefore investigate the effect of calcineurin on basal and AngII-mediated vascular remodelling with the help of a global PPP3CB knockout mouse model.[25]

2 | RESULTS

2.1 | PPP3CB KO mice and WT controls show no major differences in basal overall and vascular phenotype

There were no differences in body weight, organ weight or tibia length between PPP3CB KO and control animals under basal conditions (Figure S1A-D). Successful global KO of PPP3CB was confirmed by qPCR experiments in different organs (Figure S1E). The mRNA expression level of PPP3CA was not affected by the KO (Figure S1F), ruling out a compensatory upregulation. Volume intake and blood pressure were measured and did not differ

between WT and PPP3CB KO mice (Figure S1G,H). To exclude an effect of PPP3CB on vascular structure under basal conditions, we determined the mRNA expression of extracellular matrix proteins. We observed no changes in the expression of Col1a1, Col3a1, Col4a1 and Fn1 or in the activation pattern of the common transcription factors, that is the pCREB/CREB ratio in WT and KO mice (Figure S1I,J). Next, we investigated aortic VSMCs, which are of major importance for basal vascular tone of vessels and can be impaired in their function by vascular remodelling processes. KO of PPP3CB was confirmed by Western Blot analyses of PPP3CB and PPP3CA (Figure S2A). No major differences in morphology, cell death, proliferation or activation and expression of common calcineurin transcription factors were observed in freshly isolated VSMCs of WT and KO mice (Figure S2B-G).

2.2 | AngII induces changes in vascular morphology in WT but not in PPP3CB KO mice with altered blood pressure response

We investigated whether PPP3CB is involved in mediating the pathological effect of AngII in the cardiovascular system. After a 2-week basal assessment phase, osmotic minipumps that released a moderate dosage of AngII for 28 days were implanted in WT and KO mice. Consistent with literature, AngII-treated WT mice showed an increase in water intake compared to WT controls at the end of the treatment phase and an increase in heart weight (Figure 1A,B). There were no changes in other organ weights, suggesting heart hypertrophy without decompensation (Figure 1C,D, Figure S3A-D). Systolic blood pressure was monitored via tail-cuff measurements and showed an initial increase in WT and KO mice receiving AngII, thus confirming effectiveness of AngII-application via osmotic minipumps (Figure 1E). While the blood pressure of WT mice ascended further over the next 3 weeks, blood pressure of KO mice decreased again so that after 4 weeks, WT mice still had a significantly increased blood pressure while KO mice did not (Figure 1E,F).

Under control conditions, the wall thickness and lumen area of the aortas of WT and KO animals were comparable. AngII led to an increase in media thickness and lumen area of the aorta in WT mice while the wall-to-lumen ratio stayed the same (Figure 1G-J). Accordingly, wall tension was increased in aortas of WT mice treated with AngII compared to control animals (Figure 1K). Likewise, aortic fibrosis of the media and adventitia thickness were increased in WT animals treated with AngII (Figure S9). In KO mice, AngII was unable to induce changes in wall thickness, lumen area, wall tension or fibrosis parameters (Figure 1G-K, Figure S9), suggesting that the vascular remodelling effect of AngII is calcineurin-dependent.

2.3 | AngII induces changes in the expression of pathophysiologically relevant genes and pathways in aortas and VSMCs of WT but not PPP3CB KO mice

To assess the underlying molecular mechanisms leading to these different responses to AngII in WT and KO animals, NGS analyses of aortic samples were performed (Figure S4A,B). Only genes with FPM ≥ 5 were taken into further consideration. Genes were regarded as regulated if they had a 1.5-fold change and a Cohen's d effect size of ± 2. With these criteria, we detected 324 up-regulated and 200 down-regulated genes between WT and KO mice under basal conditions (Figure S4C,D). A gene set enrichment analysis (GSEA) with g:Profiler and GOrilla revealed no functional clustering of the regulated genes under basal conditions between WT and KO animals. These observations could be confirmed by ingenuity pathway analysis (IPA) resulting in no enriched canonical pathways, diseases or functional annotations.

In aorta of WT mice, 635 genes were up-regulated and 270 genes were down-regulated by AngII compared to control. Of these (Figure 2A), GSEA of the regulated genes showed a strong impact on extracellular matrix structural constituents, fibronectin binding and extracellular matrix binding (Figure 2A). Additionally, an effect of AngII treatment on annotations like development of vasculature/vascularization, cell movement or migration of smooth muscle cells, apoptosis and inflammation was predicted (Figure 2B, Figure S5).

In KO mice, on the other hand, only 193 were up-regulated and 245 were down-regulated by AngII (Figure 2A). Of those genes, GSEA and IPA led to no significantly enriched disease and functions annotation or upstream regulators (Figure 2B). There was little overlap between AngII-regulated genes in WT and KO mice (Figure 2A).

Our further analysis focused on genes that were PPP3CB-dependently regulated by angiotensin, that is genes regulated by AngII only in WT but not in KO mice and also not regulated under basal conditions. Overall FPMs and Cohen's d effect sizes are indicated in Figure S4D. With GSEA, using GOrilla and g:Profiler, we detected the highest enrichment concerning gene function for type III transforming growth factor beta receptor binding and GO terms associated with EMCs (Figure S6). For gene processes with an enrichment ≥ 4, GO terms concerning extracellular matrix, wound healing, actin, proliferation, TGFβ receptor signalling and immune response and lactate transport were identified (Figure S6).

To decipher the mechanism leading to the mouse phenotype of vascular remodelling with hypertension, altered distribution of extracellular matrix, cell migration, proliferation and growth were investigated further. As markers for changes in extracellular matrix, we analysed collagen 1, 3 and 4 and

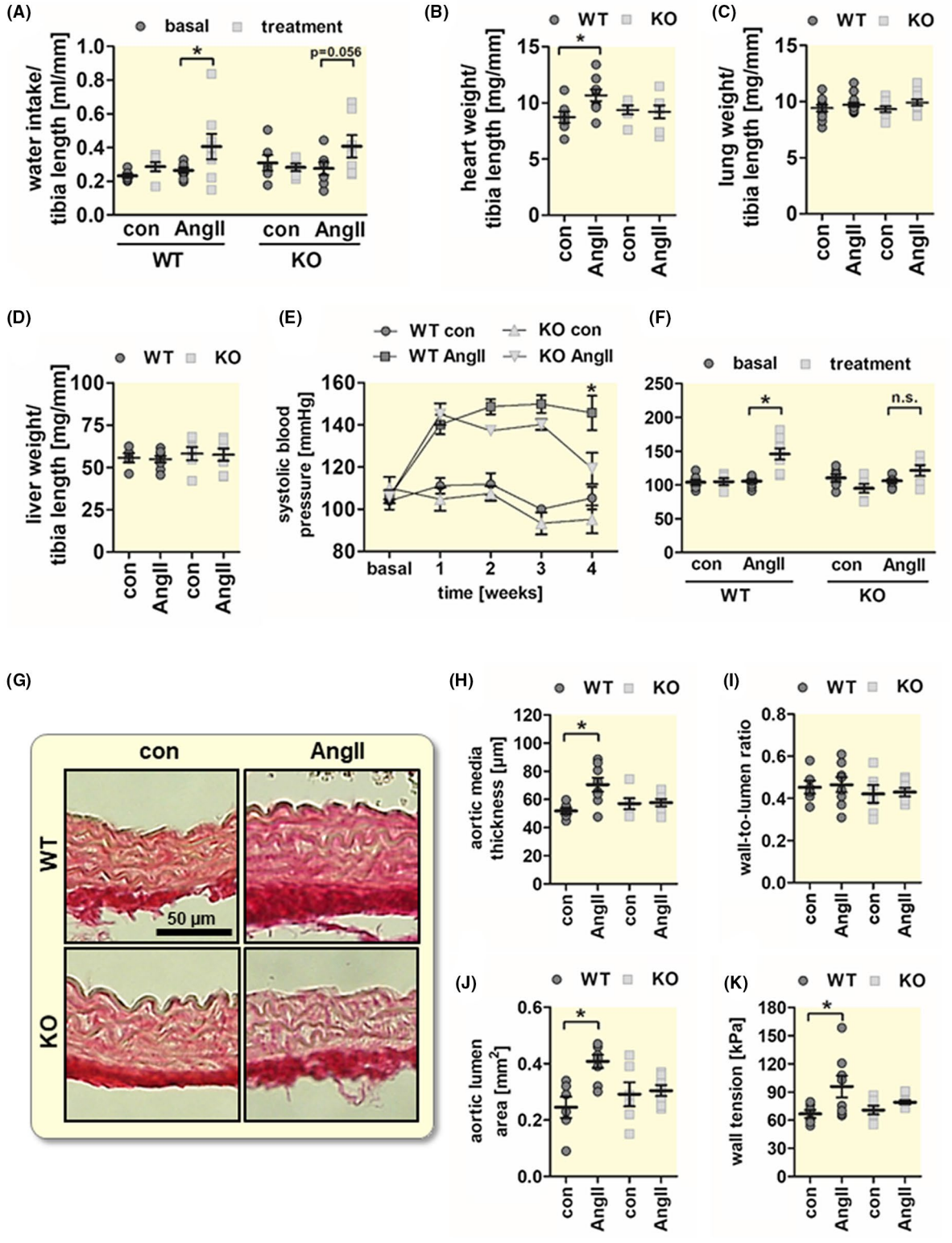

FIGURE 1 AngII-induced chronic increase in tail-cuff pressure and aortic wall remodelling are abolished by the knockout of PPP3CB. (A) Water intake of examined mice cohorts before and after 4 weeks of AngII treatment. B-D, Analysis of (B) heart weight, (C) lung weight and (D) liver weight after 4 weeks of AngII treatment (N = 6-8 per group, $*P \leq .05$). E, Time course of tail-cuff pressure measurements of WT and PPP3CB KO animals with or without chronic AngII application via osmotic minipumps (N = 6-8 per group, $*P \leq .05$). F, Comparison of tail-cuff pressures of WT and PPP3CB KO animals before and after 4 weeks of treatment with AngII (N = 6-8 per group, $*P \leq .05$). G, Representative Picro-Sirius Red stained histological aortic sections of WT and PPP3CB KO animals treated with or without chronic AngII treatment (scale bar = 50 µm). H, Quantification of aortic media thickness from control or AngII-treated male mice (N = 6-8 per group, $*P \leq .05$). I, Aortic wall-to-lumen ratio of the indicated cohorts was calculated from measurements of histological stainings (N = 6-8 per group). J, Aortic lumen area was calculated by using the inner radius (calculated from the inner circumference) of Picro-Sirius Red stained aortic sections (N = 6-8 per group, *t* test $*P \leq .05$). K, Aortic wall tension was calculated by using the law of Laplace (N = 6-8 per group, $*P \leq .05$)

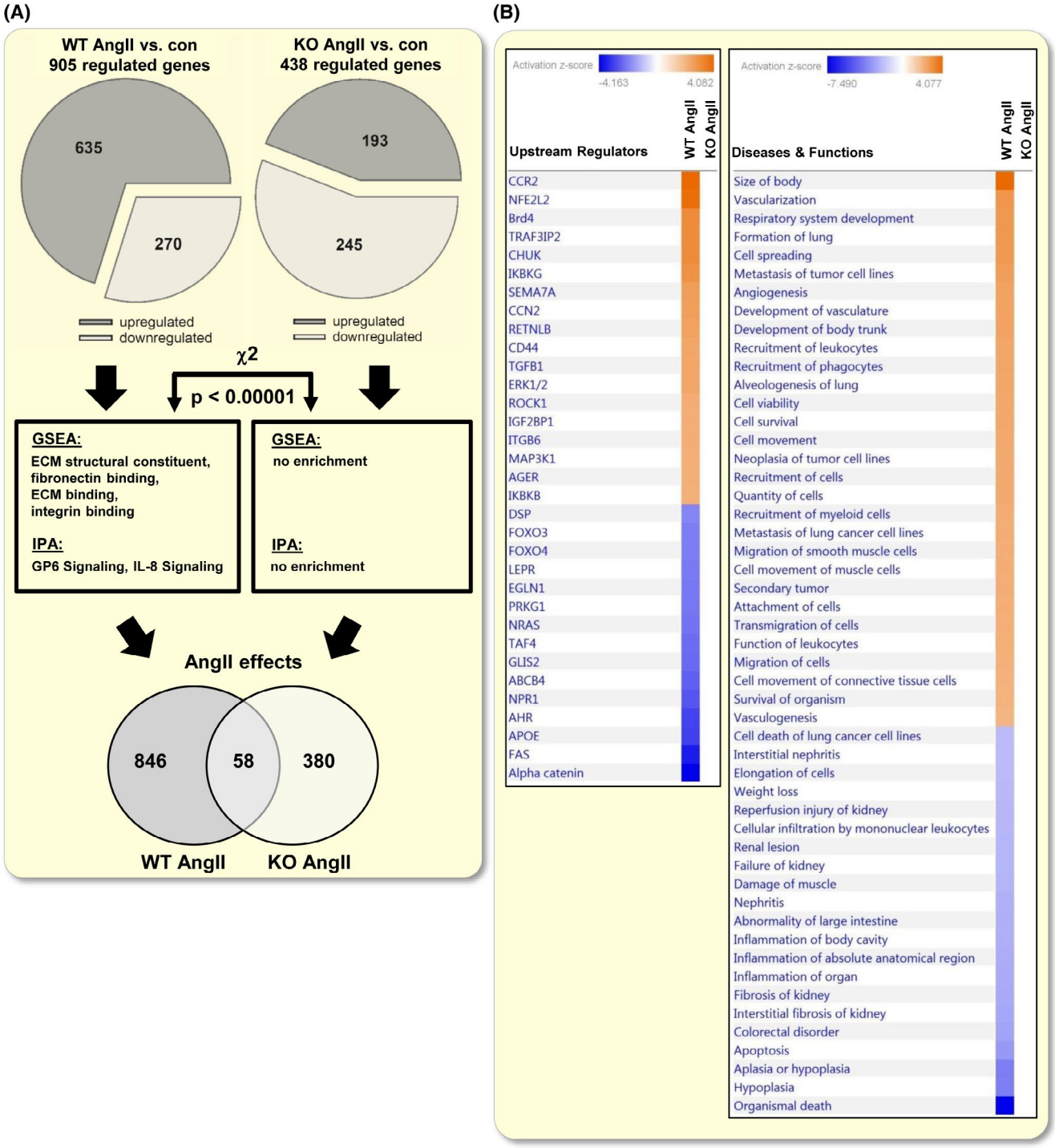

FIGURE 2 Loss of PPP3CB impairs upregulation of extracellular matrix-associated genes upon AngII treatment and relevant signalling pathways in aorta. (A, upper panel) Venn diagrams showing the number of up- and down-regulated genes of a next-generation sequencing approach with RNA samples from aorta of the previously analysed WT animals (A, left) and KO animals (A, right) after AngII stimulation compared to the respective control cohort. (A, middle panel) Both datasets were searched for enriched GO terms with GOrilla (see boxes below). The calculated chi-square statistic is 85.0556 with a $P < .00001$. (A, lower panel) Comparison of AngII-regulated genes in the two different genotypes. B, With IPA (ingenuity pathway analysis), AngII-regulated genes in WT and KO mice were compared with regard to upstream regulators and diseases and function revealing an exclusive effect of AngII in WT animals

fibronectin. We observed a significant upregulation of collagen 1, 3, 4 and fibronectin in aorta of WT animals treated with AngII with no significant response to AngII treatment in KO mice in our NGS data, which could be confirmed by qPCR validation experiments (Figure 3A-D). Further, genes associated with extracellular matrix organization

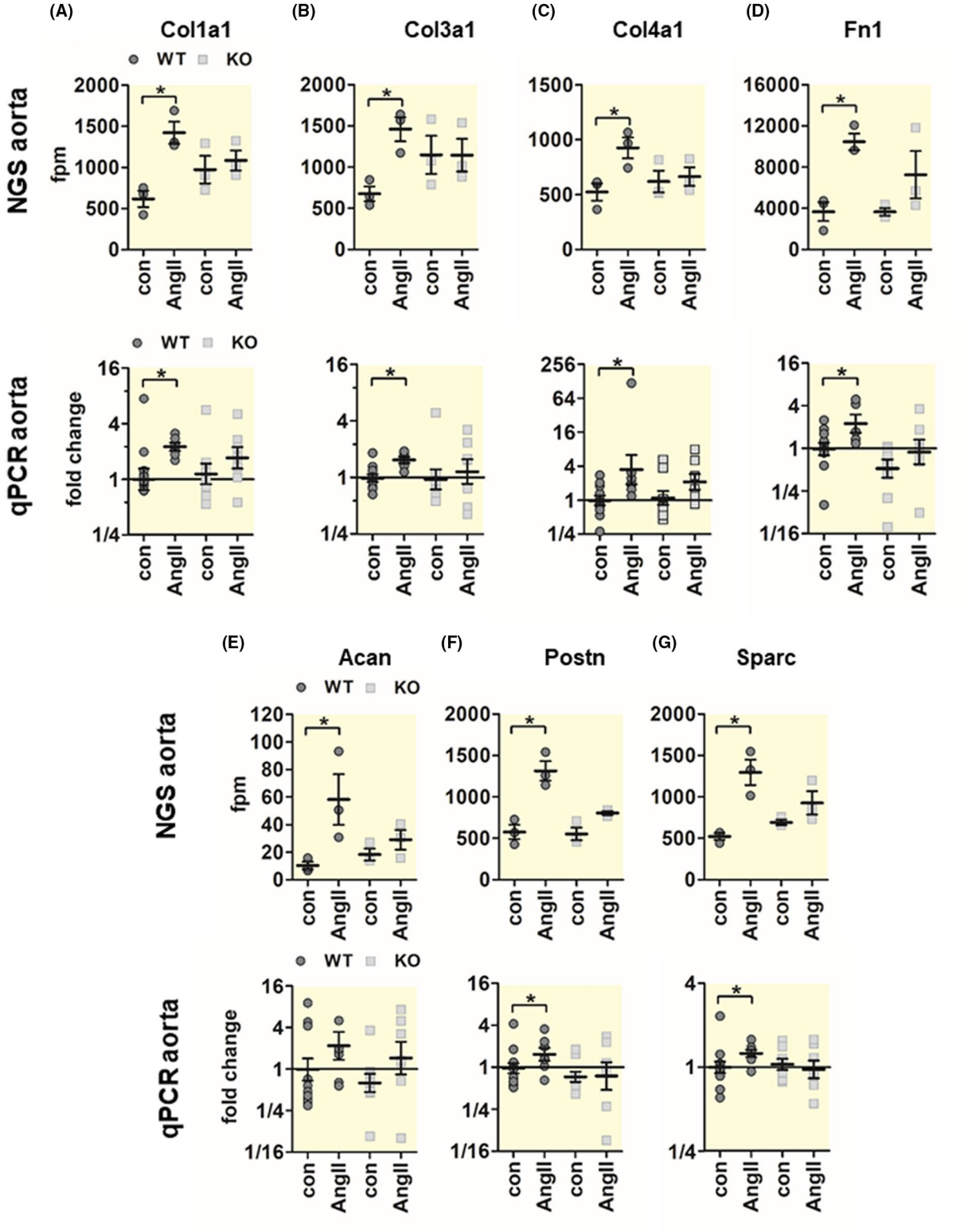

FIGURE 3 Knockout of PPP3CB abolishes increased expression of extracellular matrix-related genes after AngII-stimulation. (A-G, upper panel) Expression of extracellular matrix-associated genes that are regulated by AngII in a PPP3CB-dependent manner: results from NGS screening in fragments per million (fpm) for (A) Col1a1, (B) Col3a1, (C) Col4a1, (D) Fn1, (E) Acan, (F) Postn and (G) Sparc (n = 3 per group, $*P \leq .05$) and (lower panel A-G) corresponding qPCR experiments from aortic RNA samples (n = 6-12 per group, $*P \leq .05$)

and regulated in our NGS data by AngII in a calcineurin-dependent manner were validated by qPCR and included aggrecan (Acan), osteonectin (Sparc) and periostin (Postn) (Figure 3E-G). As additional mediators of vascular remodelling, we analysed the gene expression of plasminogen activator inhibitor 1 (Pai1), regulator of calcineurin 1 (Rcan1),

matrix metallopeptidase 2 (Mmp2) and tissue inhibitor of matrix metallopeptidase 2 (Timp2). In aorta, Pai1 and Rcan1 mRNA expression could be induced to a higher extent in WT than in PPP3CB KO mice (Figure 4A,B). No involvement of calcineurin for AngII-mediated expression for Mmp2 and Timp2 was detectable (Figure S7A,B). Furthermore, we investigated the expression of proliferation by analysing marker of proliferation ki67 (Mki67) and cyclin-dependent kinase inhibitor 1a (Cdkn1a). Only Mki67 mRNA expression was increased upon AngII treatment in WT aortae but not in the corresponding VSMCs (Figure 4C,D). This is in accordance with the results of a cell proliferation assay that reveals no differences in VSMC proliferation after AngII stimulation between the different genotypes (Figure 4E). However, we detected accelerated wound closure upon AngII treatment in WT VSMCs but not in KO cells (Figure 4F). Overall, this suggests that AngII leads to a calcineurin-dependent increase in extracellular matrix production and remodelling as well as VSMC migration but not in VSMC proliferation.

2.4 | AngII increases HBEGF expression, which leads to transactivation of the EGFR and enhanced TGFβ/CTGF signalling in WT but not PPP3CB KO mice

Next, we explored the signalling cascade leading to AngII- and calcineurin-dependent vascular remodelling. In the IPA analysis of our NGS data, TGFβ1 and CTGF (=CCN2) were predicted as upstream regulators (Figure 5A,B, upper panel). Both were directly regulated in our NGS experiments and have been previously associated with extracellular matrix remodelling and cell migration. qPCR experiments confirmed that both Tgfβ1 and Ctgf are up-regulated upon AngII treatment in aorta of WT mice. No change in extracellular matrix parameters, Tgfβ or Ctgf, was detectable in aorta of KO mice upon AngII treatment (Figure 5A,B, lower panel). In our NGS data, the expression of heparin binding epidermal growth factor like growth factor (Hbegf), which is a well-known component of the EGFR transactivation pathway, led to ERK1/2 activation and was also up-regulated upon AngII treatment in WT but not in PPP3CB KO animals (Figure 5C, upper panel). We could confirm the increased expression of HBEGF by qPCR (Figure 5C, lower panel). IPA also predicted the involvement of ERK1/2 in the regulation of gene expression. To assess if VSMCs are involved in the production of EMCs, gene expression analyses were performed in VSMCs. After AngII stimulation, Hbegf, Ctgf, Tgfβ1 and collagen 1 mRNA expression were elevated in VSMCs of WT but not of KO mice, indicating that VSMCs are involved in the calcineurin-dependent increased production of EMCs (Figure 5D-H). Losartan, an AT1 receptor inhibitor, could abrogate the induction of Col1a1, CTGF and fibronectin caused by AngII while the AT2 receptor inhibitor PD123319 had no effect (Figure 5D, Figure S8). By inhibiting TGFβ kinase with LY364947, the expressions of Col1a1, Tgfβ and Ctgf could be abolished (Figure 5E-G). Protein expression of TGFβ1, CTGF and HBEGF under basal conditions was not different between WT and KO VSMCs (Figure 6A-C) but enhanced secretion of TGFβ1, CTGF and HBEGF protein was detected upon treatment with AngII (Figure 6D-F). The secretion of CTGF could be inhibited by LY364947, confirming our mRNA results and indicating that CTGF lies downstream of TGFβ1 (Figure 6E). Furthermore, we analysed the role of HBEGF, a membrane-bound activator of EGFR signalling. Upon AngII stimulation, there was no difference in intracellular HBEGF protein in WT and KO VSMCs but in the cell culture supernatant, we could detect an increased amount of active HBEGF for WT but not for KO VSMCs (Figure 6C,F). To analyse whether activation of the EGFR results in a downstream increase in TGFβ1 and CTGF, we applied the EGFR inhibitor AG1478. Western Blot analysis in AngII-treated WT VSMCs revealed that blocking EGFR abolishes AngII-dependent increase in CTGF expression and also inhibits TGFβ1 secretion into the supernatant of WT VSMCs (Figure 6G,H). Together with our mRNA data, these results suggest that AngII-dependent PPP3CB activation increases TGFβ1 and CTGF expression via EGFR signalling. EGF as well as TGFβ1 treatment enhanced CTGF protein expression in WT VSMCs with TGFβ1 having the stronger effect (Figure 6I). CTGF secretion could be stimulated by EGF and TGFβ1 in VSMC from WT and KO animals, indicating that EGF lies downstream of PPP3 (Figure 6J). Applying a mixture of both stimuli to the cells did not further increase CTGF protein expression, suggesting that activation of the EGFR signalling leads to a stimulation of TGFβ1 signalling followed by increased CTGF expression (Figure 6I).

3 | DISCUSSION

In this study, we examined the role of the catalytic beta subunit of calcineurin (PPP3CB) in vascular remodelling mediated by AngII. Our results show that PPP3CB is necessary for vascular remodelling induced by AngII and for a sustained increase in systolic blood pressure. As underlying mechanism for these AngII-driven PPP3CB-dependent effects, we explored a new regulatory network in VSMCs that includes increased EGFR activation followed by enhanced TGFβ1 and CTGF signalling (Figure 7).

As an initial physiological AngII effect, an increased water intake of AngII-treated WT and KO animals was observed that was PPP3CB-independent. This effect is in agreement with other studies showing an increased water intake and blood pressure when activating the RAS and proves the effectiveness of our osmotic minipump system.[32,33] Additionally,

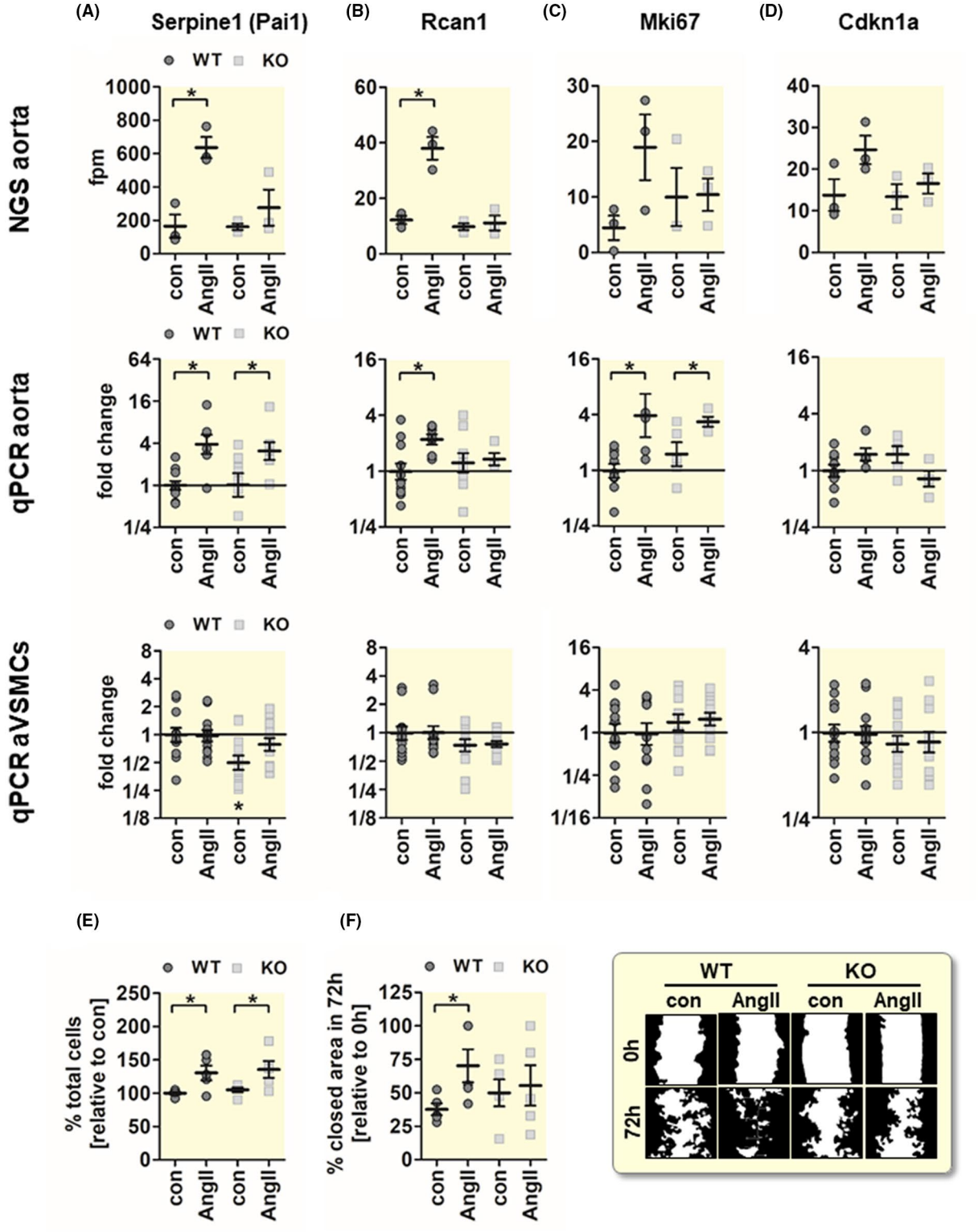

FIGURE 4 PPP3CB has an effect on AngII-dependent expression of Serpine1 (Pai1) and Rcan1 as well as on migration of VSMCs but not on proliferation. (A-D, upper panel) Expression of pathologically relevant genes in NGS analysis of murine aorta (A) Pai1, (B) Rcan1, (C) Mki67 and (D) Cdkn1a (n = 3 per group, $*P \leq .05$). (A-D, middle panel) Corresponding validation of these effects by qPCR in aortic RNA samples: (A) Pai1, (B) Rcan1, (C) Mki67 and (D) Cdkn1a (n = 4-11, $*P \leq .05$). (A-D, lower panel) qPCR analysis from WT and KO VSMCs treated with AngII was used to monitor the expression of (A) Serpine1 (Pai1), (B) Rcan1, (C) Mki67 and (D) Cdkn1a (N = 3, n = 6, $*P \leq .05$). E, The number of total cells after stimulation with AngII for 72 h was determined using a CASY Cell Counter & Analyzer (OLS Bioscience) (N = 3, n = 5, $*P \leq .05$ to respective con). (F, left panel) The percentage of closed area after applying a wound to a cell layer after 72 h was determined using light microscopy and a Fiji plugin (N = 3, n = 5, $*P \leq .05$). (F, right panel) The representative images of scratch analysis are shown as output of Fiji analysis software

we detected an AngII-induced heart hypertrophy in PPP3CB WT animals, whereas no effect was observed in KO animals. This is in accordance with literature where a calcineurin knockout suppressed cardiac hypertrophy.[25,34] Furthermore, a study from Mervaala et al[35] showed that inhibition of calcineurin via cyclosporine A prevents AngII-induced myocardial damage. Taken together, these results imply a protective role for PPP3CB KO in cardiovascular health and confirm that our moderate AngII dose is able to induce physiological and pathophysiological AngII-effects.

In aortic sections of AngII-treated PPP3CB wildtype (WT) animals, we observed an increased media thickness, lumen area and an elevated wall tension, whereas these effects were not detectable in KO animals. In several studies, it is reported that chronic AngII infusion leads to an increased vascular wall thickening.[36-38] Several mechanisms can lead to vascular remodelling caused by chronically elevated AngII levels, for example inflammation, extracellular matrix production or increased cell migration or proliferation.[22,39,40] With NGS and qPCR experiments, we could demonstrate an upregulation of fibronectin and collagen 1, 3 and 4 mRNA as well as other extracellular matrix-associated genes like aggrecan (Acan), periostin (Postn) or osteonectin (Sparc) in aortic samples of AngII-treated PPP3CB WT mice but not in KO animals. This suggests that PPP3CB-dependent wall thickening is the result of excessive extracellular matrix production. Sustained PPP3CB-dependent elevated blood pressure seems to depend on vascular remodelling processes because KO animals without media wall thickening of the aorta or changes in lumen area do not show a sustained increase in blood pressure.

In comparison to literature, we identified a lower number of AngII-regulated genes in our NGS approach. This may be due to the moderate AngII dose of 500 ng/kg/min in our study that resembles in vivo conditions.[22] In agreement with previous cyclosporine A experiments, migration of VSMCs and vessel remodelling was inhibited in our KO model, indicating that the PPP3CB subunit is relevant for regulation of VSMC migration, extracellular matrix production and vessel remodelling.[22] Compared to these experiments with a pharmacological inhibitor, our PPP3CB KO model targets calcineurin more specifically and we can rule out that unspecific side effect contributed to the detected differences.[41,42]

To unravel the signalling mechanisms leading to vascular remodelling, mRNA expression and protein secretion of WT and KO VSMCs were analysed. We measured an upregulation of Tgfβ1, Ctgf and Col1a1 mRNA expression after stimulation with AngII and a corresponding enhanced secretion of CTGF and TGFβ1 protein. Inhibition of TGFβ kinase abolished the increase in CTGF and collagen 1 induced by AngII, indicating that TGFβ1 is located upstream of CTGF and collagen 1. It is known from literature that TGFβ1 and CTGF play an essential role in fibrosis development and migration where TGFβ1 and CTGF interact in a complex manner.[43,44] For example, the CTGF promoter contains SMAD-binding elements.[45] In literature, PPP3CB already has been linked to fibrotic remodelling processes in other organs like heart and pulmonary arteries. In a cardiomyocyte-specific calcineurin deletion model, the loss of calcineurin led to a significantly reduced cardiac fibrosis.[34] In a study from de Frutos et al[46], inhibition of the calcineurin/NFaT pathway abolished pulmonary arterial wall thickening.

AngII is part of the RAS and can activate different receptors. While stimulation of AT1 receptor is known to support vascular remodelling and blood pressure increase, AT2 and Mas receptor mediate opposite effects and are known to be vasoprotective. In vivo AngII can also trigger the release of aldosterone from the adrenal glands, which causes transactivation of the mineralocorticoid receptor and mimics the effects induced by the AT1 receptor. However, pathological aldosterone effects usually require additional stress factors to be present like high salt concentrations or partial nephrectomy. In our case, signalling could be inhibited by the AT1 receptor inhibitor losartan in VSMCs so that the most likely signalling intermediate between AngII and calcineurin is the AT1 receptor.

Our Next-Generation Sequencing (NGS) and IPA results suggest that HBEGF is the missing link between AngII-mediated activation of calcineurin and increased TGFβ1 expression. In its inactive form, HBEGF is membrane-bound and is released via ectodomain shedding into the extracellular space while the HBEGF-c-terminal fragment remains in the cell.[47] HBEGF has been shown to be released after AT_1 receptor activation by AngII, leading to EGFR transactivation.[48]

The EGFR is mainly known for its role in tumorigenesis but has also been associated with AngII-mediated regulation of vascular tone and blood pressure, vascular remodelling, fibrosis, cell migration and cardiac hypertrophy.[49-52] We detected increased amounts of secreted HBEGF after AngII stimulation in WT but not in PPP3CB KO VSMCs, suggesting a role of HBEGF in EGFR transactivation in our WT model. Previous studies also demonstrate a participation of VSMCs in EGFR-dependent regulation of vascular tone and media thickening.[52] This could explain the observed effects in our PPP3CB WT animals with increased aortic media thickness and sustained systolic blood pressure. By blocking EGFR activation with AG1478, we measured a reduced TGFβ1 and CTGF secretion in VSMCs after AngII stimulation. These results support the idea that a crosstalk between EGFR and TGFβ1/CTGF signalling is calcineurin-dependent. Furthermore, we show that both signalling cascades act successively and not synergistically downstream of PPP3CB, leading to increased extracellular matrix production. In literature, it has been also described that activation of the EGFR can lead to increased CTGF expression.[53,54] These results are in accordance with a study from Liu et al[55] showing an EGFR-dependent upregulation of CTGF expression that leads to cardiac fibrosis. Subsequently,

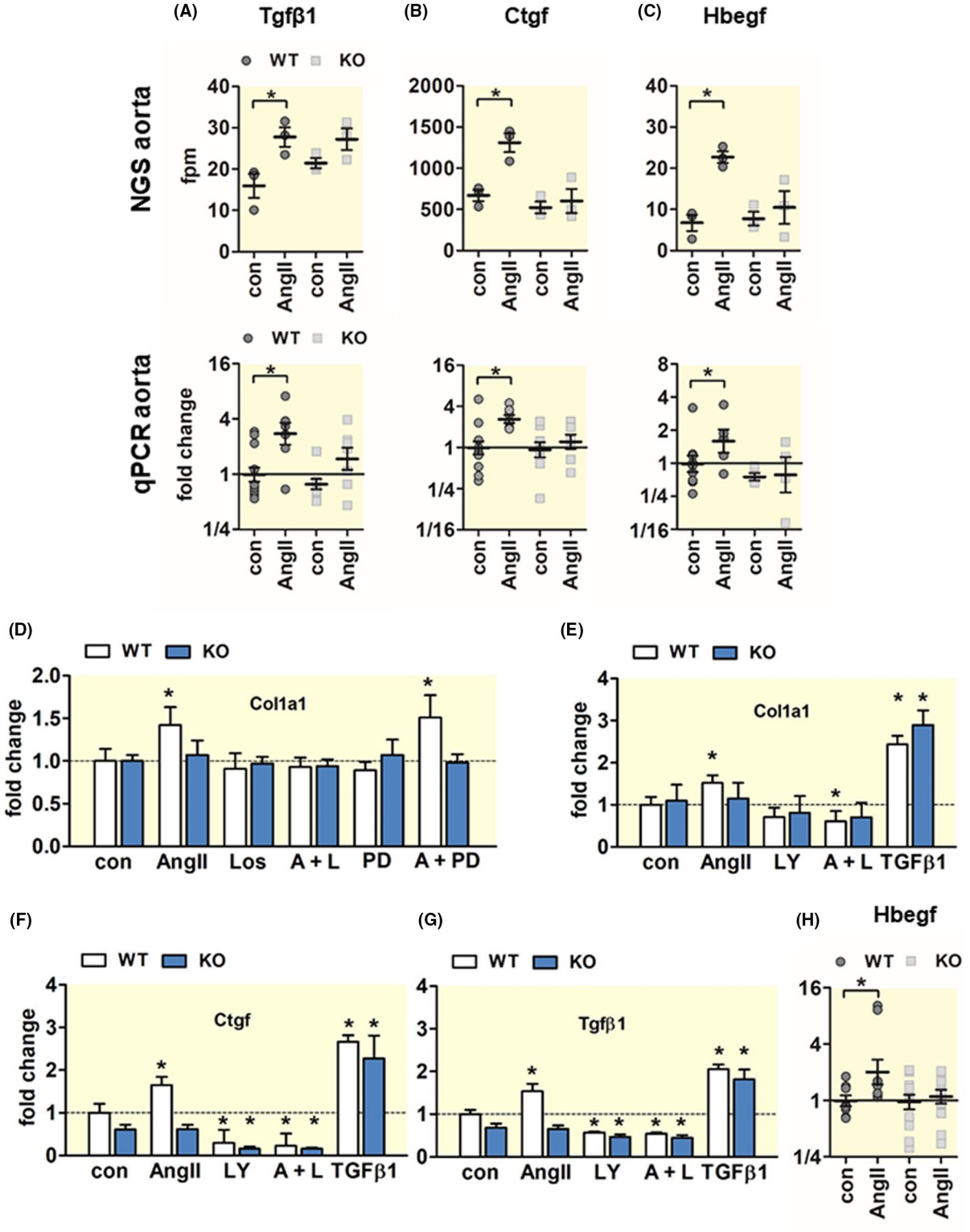

FIGURE 5 AngII-mediated expression of Col1a1, Tgfβ1, Ctgf and Hbegf is dependent on AT1 receptor and PPP3CB expression. (A-C, upper panel) Expression of genes that are regulated by AngII in a PPP3CB-dependent manner: results from NGS screening in fragments per million (fpm) for (A) Tgfβ1, (B) Ctgf and (C) Hbegf (n = 3 per group, $*P \leq .05$). (A-C, lower panel) Corresponding validation of the effects via qPCR in aortic samples (n = 5-12 per group, $*P \leq .05$). D, RNA expression analysis with qPCR in stimulated aVSMCs from WT and KO mice after treatment with 100 nM AngII, 10 μM Losartan (Los), 10 μM PD123319 (PD) or AngII+Losartan (A + L) and AngII+PD123319 (A + PD) in combination for 72 h for Col1a1 (N = 3, n = 6, $*P \leq .05$ to respective con). E-G, RNA expression analysis in stimulated VSMCs from WT and KO mice after treatment with 100 nM AngII, 5 ng/mL recombinant murine TGFβ1, 3 μM TGFβ1 inhibitor (LY364947, LY) or AngII + LY364947 (A + L) in combination for 72 h for (E) Col1a1, (F) TGFβ1 and (G) Ctgf (N = 3, n = 6, $*P \leq .05$ to respective con). H, Measurement of Hbegf mRNA expression after 72 h AngII-stimulation of VSMCs from WT and KO animals via qPCR (N = 3, n = 6; $*P \leq .05$)

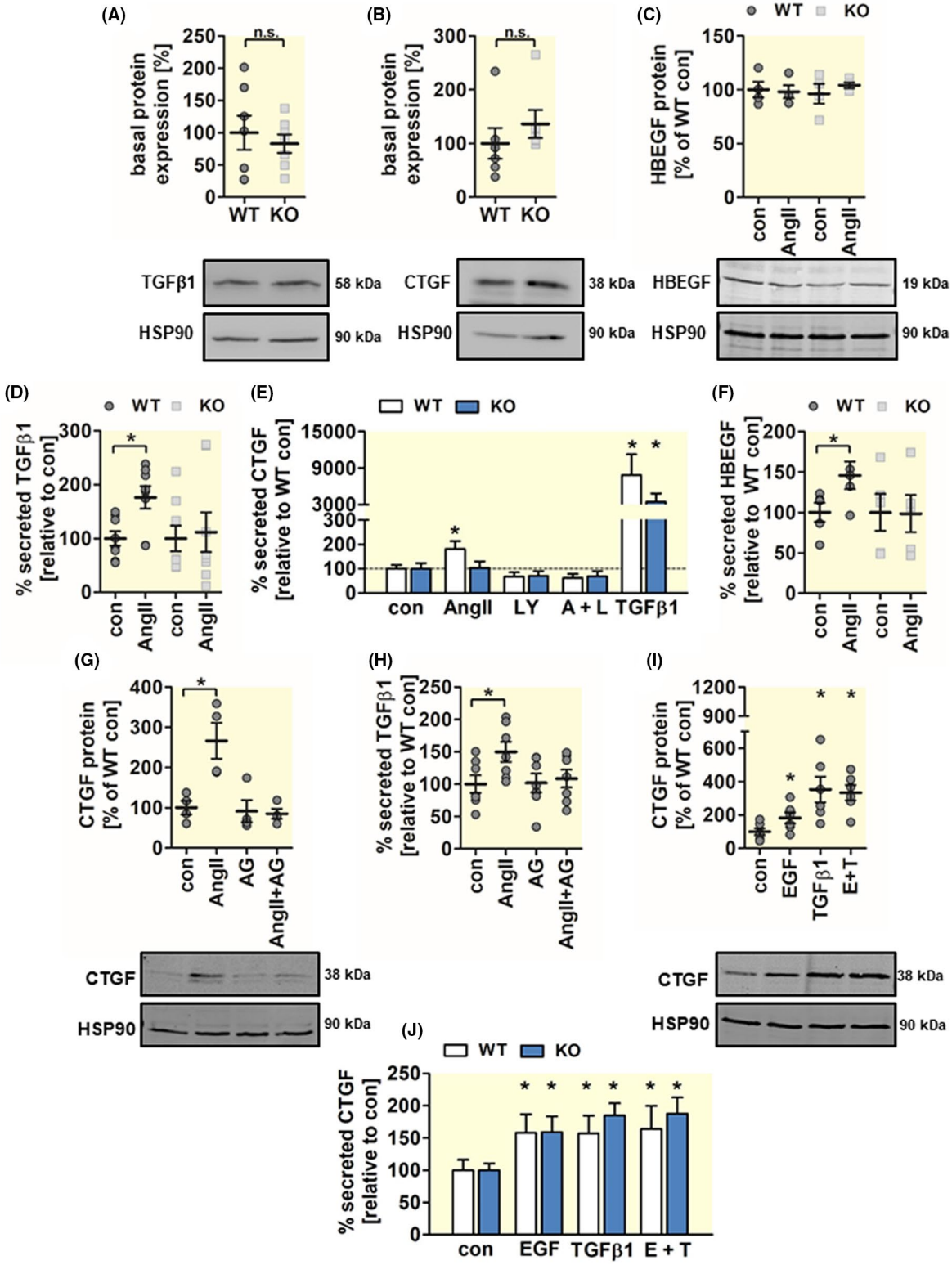

blocking EGFR activation led to reduced AngII-dependent CTGF expression. Yang et al[56] showed a direct correlation between EGFR activation by AngII via HBEGF and increased smooth muscle cell proliferation and migration. In this case, the increased proliferation led to a higher extracellular matrix production by the cells. Our study expands this model suggesting a crucial role for PPP3CB for AngII-mediated fibrosis development and vascular remodelling that is mediated by EGFR transactivation followed by enhanced TGFβ1 signalling and CTGF expression.

FIGURE 6 PPP3CB mediates AngII-dependent secretion of TGFβ1 and CTGF via increased HBEGF-driven EGFR transactivation. A,B, Representative Western Blots and corresponding quantification showing the basal expression level of (A) CTGF and (B) TGFβ1 with heat shock protein 90 (HSP90) as housekeeping protein (n = 6 per group). C, HBEGF protein content in VSMCs was determined by Western Blot after 72 h AngII-stimulation and normalized to HSP90 amount (N = 3, n = 6). D,E, Measurement of secreted (D) TGFβ1 and (E) CTGF via ELISA was performed in cell culture media from AngII-stimulated WT and KO VSMCs. In (E), cells were additionally stimulated with 3 μM TGFβ1 inhibitor (LY364947, LY), AngII + LY364947 (A + L) or 5 ng/mL recombinant murine TGFβ1 for 72h. Amount of secreted protein was normalized to whole protein content relative to 72 h WT con or KO con (N = 3, n = 6, $*P \leq .05$ to respective con). F, Quantification of secreted HBEGF was performed by ELISA in cell culture media from WT and KO VSMCs stimulated with AngII for 72 h (N = 4, n = 7, $*P \leq .05$). G, Analysis of CTGF protein expression with Western Blot in WT VSMCs after 72-h incubation with AngII and/or 1 μM AG1478 normalized to HSP90 expression (N = 4, n = 4, $*P \leq .05$ to WT con). H, Detection of secreted TGFβ1 by ELISA in cell culture media from WT VSMCs (N = 4, n = 7, $*P \leq .05$). I, Detection of CTGF protein expression by Western Blot in WT VSMCs stimulated with 10 μg/L EGF and/or 5 ng/mL recombinant TGFβ1 normalized to HSP90 expression (N = 3, n = 9, $*P \leq .05$ to WT con). J, Measurements of secreted CTGF via ELISA were performed in cell culture media from WT and KO aVSMCs stimulated with 10 μg/L EGF, 5 ng/mL recombinant murine TGFβ1 or EGF in combination with TGFβ1 (E + T) for 24 h, medium was collected and assayed according to the manufacturer's instructions. The amount of secreted protein was normalized to whole protein content relative to 24 h WT con or KO con (N = 3, n = 6, $*P \leq .05$ to respective con)

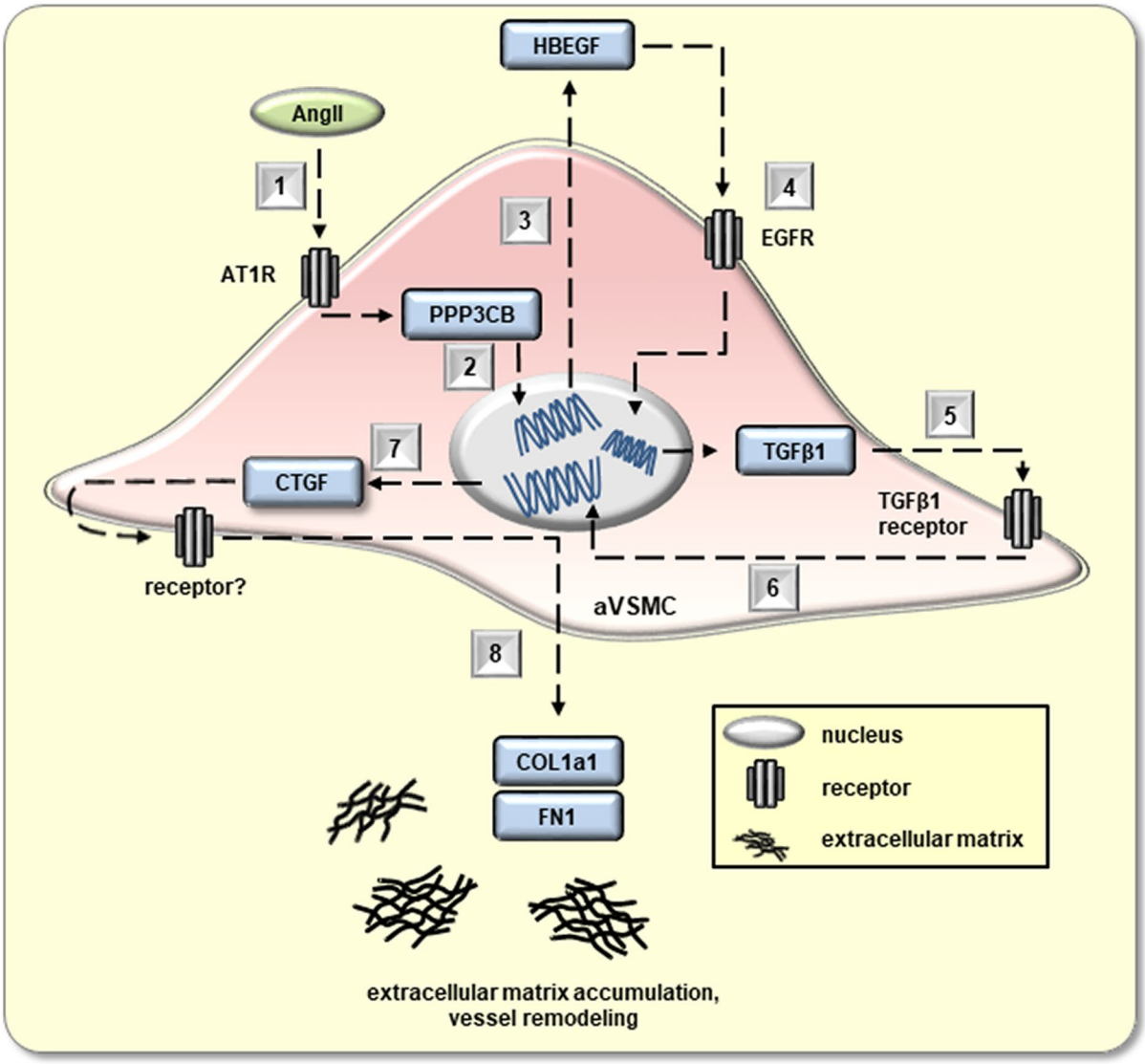

FIGURE 7 Proposed working model in VSMCs: (1) AngII-dependent activation of PPP3CB leads to (2) activation of HBEGF mRNA and protein expression and (3) increased secretion. HBEGF activates the EGFR (4), which increases the mRNA and protein expression of TGFβ1 (5) and TGFβ1 secretion. (6) TGFβ1 stimulates CTGF gene and protein expression. (7) CTGF via an unknown receptor increases (8) COL1a1 and FN1 secretion and deposition of extracellular matrix followed by pathological vessel remodelling

Our results are in accordance with the study of Wong and colleagues, where an upregulation of TGFβ1 and CTGF by AngII led to an increased fibrosis formation in heart with elevated Col1a1 mRNA levels. There, inhibition of TGFβ1 signalling down-regulated CTGF expression.[57] Furthermore, results from Gooch et al[58] showed that calcineurin activates TGFβ1 activity and thereby increases extracellular matrix production in the kidney. PPP3CA was responsible for the observed effects, but not PPP3CB, which implies that both isoforms have tissue-specific functions. As many of the studies deal with the downstream effects of elevated CTGF levels, we analysed the upstream signals mediating CTGF expression in VSMCs demonstrating a new insight in calcineurin-dependent regulation of EGFR signalling. Our in vivo and ex vivo experiments indicate that VSMCs play an important role in the observed vascular remodelling effects and we could confirm an impact of PPP3CB for AngII signalling.

Overall, our results show that pathological AngII effects in the vasculature are mediated by calcineurin via EGFR and TGFβ1/CTGF signalling (Figure 7). This may result in aortic wall remodelling with increased wall thickness and lumen area followed by elevated tail-cuff pressure in PPP3CB WT animals. In contrast, animals with a lack of PPP3CB seem to be protected against the described alterations. This implies a beneficial effect of respective inhibitors against vascular remodelling and possibly hypertension, which may be used in addition to standard RAS inhibitors in cardiovascular diseases. Additional analysis especially of blood pressure are required to validate this further.

4 | MATERIALS AND METHODS

All the material submitted conform good publishing practice in physiology.[59]

4.1 | Mouse model

Mice were purchased from Jackson laboratory (JAX; B6,129S6-Ppp3cb^{tm1Jmk}/J; stock #009066) and kept under SPF conditions.[25] Mice were kept under a 12-hour/12-hour light/dark cycle with a room temperature of 20 ± 1°C. Genotyping was performed according to JAX. Mouse experiments were performed with 5-month-old male mice and were approved by the local government (Landesverwaltungsamt Sachsen-Anhalt, permit number 42502-2-1164 MLU). All animal procedures performed conformed to the guidelines from Directive 2010/63/EU. The study was blinded and randomized.

4.2 | Harvesting of organs

Mice were sacrificed by cervical dislocation and organs were excised, carefully freed from adjacent tissue and weighed. For normalization of organ weights, tibia length was measured. Parts of the tissue were snap frozen in liquid nitrogen immediately.

4.3 | VSMC culture

Aortas were digested with collagenase II (1.5 mg/mL) for 4-6 hours at 37°C and centrifuged at 300*g* for 5 minutes. Cell pellet was resuspended in 1:1 DMEM/Ham's F12 (supplemented with 5 mg/L human apo-transferrin, 5 mg/L insulin, 36 μg/L hydrocortisone, 5 μg/L sodium selenite, 10 μg/L EGF, 10% FCS, 1% penicillin/streptomycin and 1.4 g/L glucose) and Smooth Muscle Cell Growth Medium (PELOBiotech). Cells were maintained at 37°C under humidified conditions of 95% air and 5% CO_2. For stimulation experiments, cells were maintained for 24 hours under serum starvation and incubated as indicated.

4.4 | Measurement of blood pressure with tail-cuff

Mice were trained 14 days before starting the blood pressure measurement for 5 consecutive days using external tail pulse detection (AD Instruments) in awake animals. After this time period, AngII-releasing osmotic minipumps (500 ng/kg/min; Alzet) were implanted subcutaneously in the back of the animals under isoflurane anaesthesia (2% in 100% O_2, 1 L/min). Control animals were sham-operated without minipump. After a 3-day recovery period, tail-cuff pressure was measured twice weekly for additional 28 days.

4.5 | Histological analysis

Organs were collected, fixed in 4% paraformaldehyde solution, embedded in paraffin wax and cut in 5 μm sections. Samples were stained with Picro Sirius Red. The thickness of the aortic media was determined at 10 different regions of the cross-section; additionally, inner and outer circumferences were measured to calculate wall-to-lumen ratio and aortic lumen area. The wall tension was calculated by the Laplace Law (T(wall tension) = P(blood pressure) × r(radius)/d(wall thickness)) and the pressure was taken from the tail-cuff measurements (1 mm Hg = 133,32 Pa). Aortic fibrosis was quantified by assessing Picro Sirius Red staining intensity

in the media with ImageJ Fiji and by measuring adventitia thickness in aortic cross-sections.

4.6 | Next-Generation Sequencing

Sequencing was performed at the sequencing core facility of the IZKF Leipzig (Faculty of Medicine, University Leipzig) as described in the supplements. Furthermore, gene enrichment analysis was done by GOrilla and g:Profiler.[60,61] Upstream and downstream pathway analyses were performed with the ingenuity pathway analyzer (IPA) from Qiagen.

4.7 | Western Blot

Cells or tissues were lysed in RIPA buffer followed by centrifugation for 10 minutes with 13 800 *g*. Supernatant was transferred to a new tube and protein content was determined by BCA assay. Equal amounts of protein were separated by 10% SDS-PAGE, transferred to nitrocellulose membrane and incubated with primary antibodies at 4°C with gentle shaking overnight as indicated in Table S2. The membranes were then incubated with secondary antibody for 2 hours as indicated in Table S2. Antibodies were validated with the help of a positive control (ie, recombinant protein or tissue lysates/cell lysates with known high expression of target genes) and by comparing the band to a molecular weight marker. Only antibodies that yielded a distinct single band of the expected height were used for further experiments. Protein bands were detected in the linear range with an ImageQuant System (GE Healthcare) or visualized using a LI-COR Odyssey Imaging System.

4.8 | ELISA

Cells were incubated in serum-free media and stimulated as indicated. Secreted CTGF, TGFβ1 and HBEGF were measured in the media according to the manufacturer's instructions (LSBio and R&D Systems) and normalized to cellular protein content. The following kits were used: Mouse CTGF ELISA Kit; LSBio; LS-F30605; DuoSet ELISA mouse HBEGF; R&D Systems; DY8239-05; DuoSet ELISA mouse TGFβ1; R&D Systems; DY1679-05.

4.9 | Assessment of cell proliferation and migration

Cell proliferation was determined by using a CASY Cell Counter & Analyzer (OLS). Cell migration was assessed by applying a wound to a cell layer and analysis of corresponding bright field images after 72 hours with a Fiji plugin.

4.10 | qPCR

For detailed information, see supplemental methods section.

4.11 | Statistics

For statistical analysis, Sigma Plot 12 or GraphPad Prism was used. After successful normality test (Shapiro-Wilk), ANOVA analysis was performed with Holm-Sidak or Dunnett's post hoc test. When just two groups were compared, student's *t* test was used. If data were not normally distributed, Wilcoxon matched-pairs signed rank test was used. Differences were considered significant at values of $P \leq .05$. For evaluating NGS data distribution, chi square test was used.

ACKNOWLEDGEMENTS

The work was supported by the Wilhelm Roux Programm of the Martin Luther University Halle-Wittenberg and the Deutsche Forschungsgemeinschaft (DFG) grant GE 905/19-1. We thank Michael Kopf for excellent technical assistance.

CONFLICTS OF INTEREST

The authors have no conflicts of interest to declare.

ORCID

Claudia Grossmann https://orcid.org/0000-0003-2026-1980

REFERENCES

1. Lacolley P, Regnault V, Nicoletti A, Li Z, Michel J-B. The vascular smooth muscle cell in arterial pathology: a cell that can take on multiple roles. *Cardiovasc Res*. 2012;95(2):194-204.
2. van Thiel Bibi S, van der Pluijm I, te Riet L, Essers J, Danser AHJ. The renin–angiotensin system and its involvement in vascular disease. *Eur J Pharmacol*. 2015;76:3-14.
3. Unger T. The role of the renin-angiotensin system in the development of cardiovascular disease. *Am J Cardiol*. 2002;89(2):3-9.
4. Chen X-L, Tummala PE, Olbrych MT, Alexander RW, Medford RM. Angiotensin II induces monocyte chemoattractant protein-1 gene expression in rat vascular smooth muscle cells. *Circ Res*. 1998;83(9):952-959.
5. Fu Z, Wang M, Gucek M, et al. Milk fat globule protein epidermal growth factor-8. *Circ Res*. 2009;104(12):1337-1346.
6. Wang M, Zhang J, Spinetti G, et al. Angiotensin II activates matrix metalloproteinase type II and mimics age-associated carotid arterial remodeling in young rats. *Am J Pathol*. 2005;167(5):1429-1442.
7. Patel VB, Zhong J, Fan D Angiotensin-converting enzyme 2 Is a critical determinant of angiotensin-induced loss of vascular smooth

muscle cells and adverse vascular remodeling. *Hypertension*. 2014;64(1):157-164.
8. Sharma RK, Desai R, Waisman DM, Wang JH. Purification and subunit structure of bovine brain modulator binding protein. *J Biol Chem*. 1979;254(10):4276-4282.
9. Wang JH, Desai R. Modulator binding protein. Bovine brain protein exhibiting the Ca2+-dependent association with the protein modulator of cyclic nucleotide phosphodiesterase. *J Biol Chem*. 1977;252(12):4175-4184.
10. Rusnak F, Mertz P. Calcineurin: form and function. *Physiol Rev*. 2000;80(4):1483-1521.
11. Shibasaki F, Hallin U, Uchino H. Calcineurin as a multifunctional regulator. *J Biochem*. 2002;131(1):1-15.
12. Aitken A, Klee CB, Cohen P. The structure of the B subunit of calcineurin. *Eur J Biochem*. 1984;139(3):663-671.
13. Lee B, Cao R, Choi YS, et al. The CREB/CRE transcriptional pathway: protection against oxidative stress-mediated neuronal cell death. *J Neurochem*. 2009;108(5):1251-1265.
14. Mair W, Morantte I, Rodrigues AP, et al. Lifespan extension induced by AMPK and calcineurin is mediated by CRTC-1 and CREB. *Nature*. 2011;470(7334):404-408.
15. Bueno OF, Brandt EB, Rothenberg ME, Molkentin JD. Defective T cell development and function in calcineurin Aß-deficient mice. *Proc Natl Acad Sci USA*. 2002;99(14):9398-9403.
16. Courtwright A, Siamakpour-Reihani S, Arbiser JL, et al. Secreted frizzle-related protein 2 stimulates angiogenesis via a calcineurin/NFAT signaling pathway. *Cancer Res*. 2009;69(11):4621-4628.
17. Graef IA, Chen F, Chen L, Kuo A, Crabtree GR. Signals transduced by Ca(2+)/calcineurin and NFATc3/c4 pattern the developing vasculature. *Cell*. 2001;105(7):863-875.
18. Klee CB, Ren H, Wang X. Regulation of the calmodulin-stimulated protein phosphatase, calcineurin. *J Biol Chem*. 1998;273(22):13367-13370.
19. Parsons SA, Wilkins BJ, Bueno OF, Molkentin JD. Altered skeletal muscle phenotypes in calcineurin Aalpha and Abeta gene-targeted mice. *Mol Cell Biol*. 2003;23(12):4331-4343.
20. Schulz RA, Yutzey KE. Calcineurin signaling and NFAT activation in cardiovascular and skeletal muscle development. *Dev Biol*. 2004;266(1):1-16.
21. Fujiwara M, Hasebe T, Kajita M, Ishizuya-Oka A, Ghazizadeh M, Kawanami O. RCAN1 regulates vascular branching during Xenopus laevis angiogenesis. *J Vasc Res*. 2011;48(2):104-118.
22. Esteban V, Mendez-Barbero N, Jimenez-Borreguero LJ, et al. Regulator of calcineurin 1 mediates pathological vascular wall remodeling. *J Exp Med*. 2011;208(10):2125-2139.
23. Mendez-Barbero N, Esteban V, Villahoz S, et al. A major role for RCAN1 in atherosclerosis progression. *EMBO Mol Med*. 2013;5(12):1901-1917.
24. Nishiyama A, Kobori H, Fukui T, et al. Role of angiotensin II and reactive oxygen species in cyclosporine A-dependent hypertension. *Hypertension*. 2003;42(4):754-760.
25. Bueno OF, Wilkins BJ, Tymitz KM, et al. Impaired cardiac hypertrophic response in Calcineurin Abeta-deficient mice. *Proc Natl Acad Sci USA*. 2002;99(7):4586-4591.
26. Bueno OF, Lips DJ, Kaiser RA, et al. Calcineurin A-beta gene targeting predisposes the myocardium to acute ischemia-induced apoptosis and dysfunction. *Circ Res*. 2004;94(1):91-99.
27. Heeneman S, Sluimer JC, Daemen MJ. Angiotensin-converting enzyme and vascular remodeling. *Circ Res*. 2007;101(5):441-454.
28. Li Y, Levesque LO, Anand-Srivastava MB. Epidermal growth factor receptor transactivation by endogenous vasoactive peptides contributes to hyperproliferation of vascular smooth muscle cells of SHR. *Am J Physiol Heart Circ Physiol*. 2010;299(6):H1959-H1967.
29. Daub H, Weiss FU, Wallasch C, Ullrich A. Role of transactivation of the EGF receptor in signalling by G-protein-coupled receptors. *Nature*. 1996;379(6565):557-560.
30. Shah BH, Catt KJ. A central role of EGF receptor transactivation in angiotensin II -induced cardiac hypertrophy. *Trends Pharmacol Sci*. 2003;24(5):239-244.
31. Mazak I, Fiebeler A, Muller DN, et al. Aldosterone potentiates angiotensin II-induced signaling in vascular smooth muscle cells. *Circulation*. 2004;109(22):2792-2800.
32. Coble JP, Cassell MD, Davis DR, Grobe JL, Sigmund CD. Activation of the renin-angiotensin system, specifically in the subfornical organ is sufficient to induce fluid intake. *Am J Physiol Regul Integr Comp Physiol*. 2014;307(4):R376-R386.
33. Lazartigues E, Sinnayah P, Augoyard G, Gharib C, Johnson AK, Davisson RL. Enhanced water and salt intake in transgenic mice with brain-restricted overexpression of angiotensin (AT1) receptors. *Am J Physiol Regul Integr Comp Physiol*. 2008;295(5):R1539-R1545.
34. Martinez-Martinez S, Lozano-Vidal N, Lopez-Maderuelo MD, Jimenez-Borreguero LJ, Armesilla AL, Redondo JM. Cardiomyocyte calcineurin is required for the onset and progression of cardiac hypertrophy and fibrosis in adult mice. *FEBS J*. 2019;286(1):46-65.
35. Mervaala E, Muller DN, Park JK, et al. Cyclosporin A protects against angiotensin II-induced end-organ damage in double transgenic rats harboring human renin and angiotensinogen genes. *Hypertension*. 2000;35(1 Pt 2):360-366.
36. Brouwers-Ceiler DL, Nelissen-Vrancken HJ, Smits JF, De Mey JG. The influence of angiotensin II-induced increase in aortic wall mass on compliance in rats in vivo. *Cardiovasc Res*. 1997;33(2):478-484.
37. Stassen FR, Raat NJ, Brouwers-Ceiler DL, Fazzi GE, Smits JF, De Mey JG. Angiotensin II induces media hypertrophy and hyperreactivity in mesenteric but not epigastric small arteries of the rat. *J Vasc Res*. 1997;34(4):289-297.
38. Williams HC, Ma J, Weiss D, Lassegue B, Sutliff RL, San MA. The cofilin phosphatase slingshot homolog 1 restrains angiotensin II-induced vascular hypertrophy and fibrosis in vivo. *Lab Invest*. 2019;99(3):399-410.
39. Forrester SJ, Elliott KJ, Kawai T, et al. Caveolin-1 deletion prevents hypertensive vascular remodeling induced by angiotensin II. *Hypertension*. 2017;69(1):79-86.
40. Zhao Y, Shang F, Shi W, et al. Angiotensin II receptor type 1 antagonists modulate vascular smooth muscle cell proliferation and migration via AMPK/mTOR. *Cardiology*. 2019;143(1):1-10.
41. Laupacis A, Keown PA, Ulan RA, McKenzie N, Stiller CR. Cyclosporin A: a powerful immunosuppressant. *Can Med Assoc J*. 1982;126(9):1041-1046.
42. Lim HW, De Windt LJ, Mante J, et al. Reversal of cardiac hypertrophy in transgenic disease models by calcineurin inhibition. *J Mol Cell Cardiol*. 2000;32(4):697-709.
43. Sakai N, Nakamura M, Lipson KE, et al. Inhibition of CTGF ameliorates peritoneal fibrosis through suppression of fibroblast and myofibroblast accumulation and angiogenesis. *Sci Rep*. 2017;7(1):5392.
44. Li G, Xie Q, Shi Y, et al. Inhibition of connective tissue growth factor by siRNA prevents liver fibrosis in rats. *J Gene Med*. 2006;8(7):889-900.

45. Chen Y, Blom IE, Sa S, Goldschmeding R, Abraham DJ, Leask A. CTGF expression in mesangial cells: involvement of SMADs, MAP kinase, and PKC. *Kidney Int*. 2002;62(4):1149-1159.
46. de Frutos FS, Spangler R, Alo D, Bosc LV. NFATc3 mediates chronic hypoxia-induced pulmonary arterial remodeling with alpha-actin up-regulation. *J Biol Chem*. 2007;282(20):15081-15089.
47. Higashiyama S, Nanba D, Nakayama H, Inoue H, Fukuda S. Ectodomain shedding and remnant peptide signalling of EGFRs and their ligands. *J Biochem*. 2011;150(1):15-22.
48. Mifune M, Ohtsu H, Suzuki H, et al. G protein coupling and second messenger generation are indispensable for metalloprotease-dependent, heparin-binding epidermal growth factor shedding through angiotensin II type-1 receptor. *J Biol Chem*. 2005;280(28):26592-26599.
49. Chan SL, Umesalma S, Baumbach GL. Epidermal growth factor receptor is critical for angiotensin II-mediated hypertrophy in cerebral arterioles. *Hypertension*. 2015;65(4):806-812.
50. Hao L, Du M, Lopez-Campistrous A, Fernandez-Patron C. Agonist-induced activation of matrix metalloproteinase-7 promotes vasoconstriction through the epidermal growth factor-receptor pathway. *Circ Res*. 2004;94(1):68-76.
51. Kagiyama S, Eguchi S, Frank GD, Inagami T, Zhang YC, Phillips MI. Angiotensin II-induced cardiac hypertrophy and hypertension are attenuated by epidermal growth factor receptor antisense. *Circulation*. 2002;106(8):909-912.
52. Schreier B, Hunerberg M, Mildenberger S, et al. Deletion of the EGF receptor in vascular smooth muscle cells prevents chronic angiotensin II-induced arterial wall stiffening and media thickening. *Acta Physiol*. 2018;222(3):e12996.
53. Chen HY, Lin CH, Chen BC. ADAM17/EGFR-dependent ERK activation mediates thrombin-induced CTGF expression in human lung fibroblasts. *Exp Cell Res*. 2018;370(1):39-45.
54. Rayego-Mateos S, Morgado-Pascual JL, Rodrigues-Diez RR, et al. Connective tissue growth factor induces renal fibrosis via epidermal growth factor receptor activation. *J Pathol*. 2018;244(2):227-241.
55. Liu X, Lin L, Li Q, et al. ERK1/2 communicates GPCR and EGFR signaling pathways to promote CTGF-mediated hypertrophic cardiomyopathy upon Ang-II stimulation. *BMC Mol Cell Biol*. 2019;20(1):14.
56. Yang X, Zhu MJ, Sreejayan N, Ren J, Du M. Angiotensin II promotes smooth muscle cell proliferation and migration through release of heparin-binding epidermal growth factor and activation of EGF-receptor pathway. *Mol Cells*. 2005;20(2):263-270.
57. Wong CKS, Falkenham A, Myers T, Legare JF. Connective tissue growth factor expression after angiotensin II exposure is dependent on transforming growth factor-beta signaling via the canonical Smad-dependent pathway in hypertensive induced myocardial fibrosis. *J Renin Angiotensin Aldosterone Syst*. 2018;19(1):1470320318759358.
58. Gooch JL, Roberts BR, Cobbs SL, Tumlin JA. Loss of the alpha-isoform of calcineurin is sufficient to induce nephrotoxicity and altered expression of transforming growth factor-beta. *Transplantation*. 2007;83(4):439-447.
59. Persson PB. Good publication practice in physiology 2019. *Acta Physiol*. 2019;227(4):e13405.
60. Eden E, Navon R, Steinfeld I, Lipson D, Yakhini Z. GOrilla: a tool for discovery and visualization of enriched GO terms in ranked gene lists. *BMC Bioinformatics*. 2009;10:48.
61. Reimand J, Kull M, Peterson H, Hansen J, Vilo J. g:Profiler—a web-based toolset for functional profiling of gene lists from large-scale experiments. *Nucleic Acids Res*. 2007;35(suppl_2):W193-W200.

SUPPORTING INFORMATION

Additional supporting information may be found online in the Supporting Information section.

How to cite this article: Nolze A, Köhler C, Ruhs S, et al. Calcineurin (PPP3CB) regulates angiotensin II-dependent vascular remodelling by potentiating EGFR signalling in mice. *Acta Physiol*. 2021;233:e13715. https://doi.org/10.1111/apha.13715